



Cite this: *Phys. Chem. Chem. Phys.*,
2016, **18**, 2202

R vs. *S* fluoroproline ring substitution: *trans/cis* effects on the formation of b_2 ions in gas-phase peptide fragmentation†

Matthew C. Bernier,^a Julia Chamot-Rooke^b and Vicki H. Wysocki^{*a}

The b_2 structures of model systems Xxx-Flp-Ala (Flp = 4*R*-fluoroproline) and Xxx-flp-Ala (flp = 4*S*-fluoroproline) (where Xxx is Val or Tyr) were studied by action IRMPD spectroscopy. Proline ring substitutions influence the *trans/cis* isomerization of the precursor ion, resulting in different b_2 fragment ion structures by collision induced dissociation. Vibrational spectra of the b_2 ions of Val-Flp and Val-flp exhibit highly intense bands at $\sim 1970\text{ cm}^{-1}$, revealing that the dominant ion in each case is an oxazolone. The major difference between the spectra of b_2 ions for *R* vs. *S* fluoroproline is a collection of peaks at 1690 and 1750 cm^{-1} , characteristic of a diketopiperazine structure, which were only present in the 4*S*-fluoroproline (flp) cases. This suggests only one b_2 ion structure (oxazolone) is being formed for Flp-containing peptides, whereas flp-containing peptides produce a mixture of a dominant oxazolone with a lower population of diketopiperazine. In solution, Flp is known to possess a higher *trans* percentage in the N-terminally adjacent peptide bond, with flp inducing a greater proportion of the *cis* conformation. The diketopiperazine formation observed here correlates directly with the $K_{\text{trans/cis}}$ trend previously shown in solution, highlighting that the *trans/cis* isomerization likelihood for proline residues modified in the 4th position is retained in the gas-phase.

Received 28th August 2015,
Accepted 7th December 2015

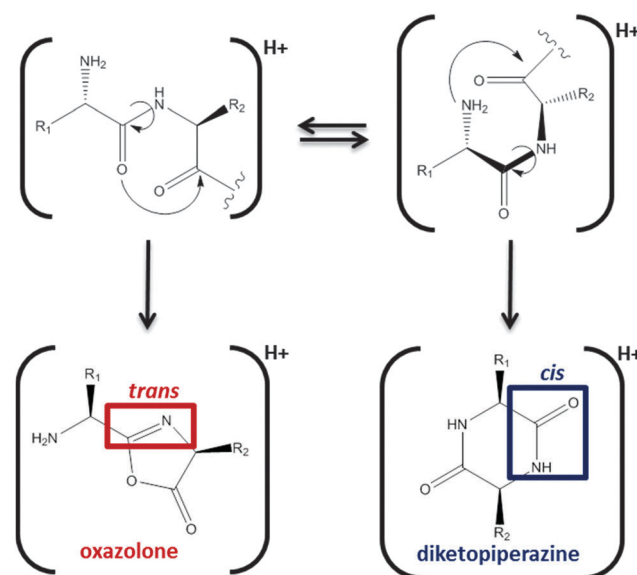
DOI: 10.1039/c5cp05155j

www.rsc.org/pccp

Introduction

In the field of peptide fragmentation, the b ion structures formed *via* collision induced dissociation (CID) have been well characterized for several sequences. CID induces fragmentation along the peptide backbone at the peptide bond, and when this bond is cleaved charge can be retained either C-terminally to the dissociated peptide bond to form a y -ion or N-terminally of this bond to form a b -ion. While y -ions are truncated peptides, b -ions must adopt variable structures to adapt to a C-terminus without a hydroxyl group. In the case of the b_2 ion, cyclization allows formation of either a five-membered oxazolone ring, in which the peptide bond retains its *trans* conformation, or a six-membered head-to-tail cyclized diketopiperazine structure (Scheme 1). To form the diketopiperazine, the peptide bond must undergo a *trans/cis* isomerization and, despite calculations that show that the diketopiperazine is typically the more stable ion, the formation of the kinetically-favored oxazolone fragment is more frequently observed.¹ This is believed to be at least in part due to the unfavorable *cis* conformation, but has also been proposed to result from the relative barriers of ring closure between oxazolone and diketopiperazine.²

The amino acid proline favors the formation of the *cis* peptide bond more than any other natural amino acid.^{4,5}



Scheme 1 Depiction of the formation of oxazolone and diketopiperazine structures for the b_2 ion. The oxazolone b_2 ions retain the *trans* amide bond conformation of the original peptide precursor while the diketopiperazine b_2 ions must form *via* a *cis* amide bond.³

^a Ohio State University, Columbus, Ohio, USA. E-mail: wysocki.11@osu.edu

^b Institut Pasteur, Paris, France

† Electronic supplementary information (ESI) available. See DOI: 10.1039/c5cp05155j

On average for protein amino acid residues, the barrier to *trans/cis* isomerization of the peptide bond adjacent to the N-terminus is approximately 20 kcal mol⁻¹, while for proline, this barrier is only 13 kcal mol⁻¹.⁶ Additionally, the relative energies between the *trans* and *cis* isomers is about 2 kcal mol⁻¹ less for proline in comparison to other residues. The lower barrier to isomerization allows b ions with a proline residue to form the diketopiperazine with greater frequency as can be observed in previous work. Gucinski *et al.* observed that the b ion structure of Val-Pro, Ala-Pro, and Ile-Pro are all mixtures of oxazolone and diketopiperazine and His-Pro is exclusively diketopiperazine.^{7,8} It was concluded in that work that the *trans/cis* isomerization barrier was an influential factor in the formation of the diketopiperazine for these systems. Furthermore, the exclusive diketopiperazine for His-Pro was determined to be a result of both the basic His residue in the first position and the second position proline contributing to *cis* stability of the peptide.

The effect of substitution of the prolyl ring on *trans/cis* propensity has been examined predominantly in the solution-phase. For example, it is well known that collagen contains 4-hydroxyproline (Hyp) and, significantly, this amino acid modification in the repeating collagen unit provides stability to the collagen triple helix. Raines and coworkers have shown that inserting other substituents (*i.e.*, fluorine and methyl) onto the prolyl rings in the Pro-Hyp-Gly motif can increase the melting temperature of the construct by over 20 °C compared to standard collagen.^{9,10} Further research by Raines and coworkers has also considered the isolated effects of proline substitution on *trans/cis* isomerization. In the case of a single acetylated and O-methylated (Ac-Xxx-OMe) form where Xxx is a substituted Pro, the $K_{trans/cis}$ value of the acetyl-Xxx peptide bond was shown to change significantly with different substituents placed in the *R* or *S* position. Using 1-D proton NMR, the $K_{trans/cis}$ of Pro was found to be 4.6. This ratio increased to 6.7 when a fluorine substituent at the 4-position was in the *R* configuration and decreased to 2.5 with fluorine in the *S* configuration.

The *trans/cis* character of each prolyl substitution was suggested, in these studies, to be directly influenced by the puckering of the prolyl ring. When in the *S* position, H, OH,

or F puckers the ring toward the adjacent peptide bond to produce the *C^γ-endo* conformation. In the *trans* position, OH or F causes the ring to pucker away from the peptide bond into the *C^γ-exo* conformation.¹¹⁻¹⁴ This effect is represented in Fig. 1, highlighting the four peptides studied in this experiment. For Tyr-flp-Ala and Val-flp-Ala (Fig. 1a and b), where fluorine is in the *S* position, the ring is puckered into the *C^γ-endo* conformation while for Tyr-Flp-Ala and Val-Flp-Ala (Fig. 1c and d), the fluorine is in the *R* position and the prolyl ring is puckered downward into the *C^γ-exo* position. The relationship of ring pucker to *trans* isomer favorability has been explained by the *gauche* effect of the downwards *C^γ-exo* puckering producing a hydrogen bonding interaction between the carbonyl in the peptide bond N-terminally adjacent locking the *trans* conformation into place. Another study by Crestoni *et al.* showed that the ions of the *R* and *S* 4-hydroxyproline amino acid (Hyp and hyp) could be distinguished using gas-phase vibrational spectroscopy, with a blue shift of the carbonyl stretching mode for the *S* configuration,¹⁵ and more recently Flick *et al.* were able to distinguish the same two *via* ion mobility of their sodium and lithium adducts.¹⁶ Along with this discovery they also noted that the *C^γ* ring puckering for these gas-phase ions followed the same trend as found for collagen in solution.

Here the model systems Tyr-flp-Ala, Tyr-Flp-Ala, Val-flp-Ala, and Val-Flp-Ala were studied, in order to test the effects of Flp and flp in the second position within a peptide. Tyr and Val were chosen as the first amino acids, as valine is known to produce a mixture of oxazolone and diketopiperazine structures in b₂ ions and tyrosine was also studied as it offers a non-basic phenyl group with very different properties from the imidazole side chain of histidine, whose effects on b-ion formation result in an overwhelming proportion of diketopiperazine.¹⁷ Furthermore, Tyr has previously been shown to influence *trans/cis* character when N-terminally adjacent to proline.¹⁸ As peptide bond isomerization is necessary for producing the diketopiperazine, the *trans* to *cis* tendency of each fluoro substituted peptide may correlate with the proportions of oxazolone and diketopiperazine in each b₂ ion population. We test here whether loss or enhancement of the diketopiperazine character for each substitution is indicative of the system's gas-phase peptide *trans/cis* bond preference.

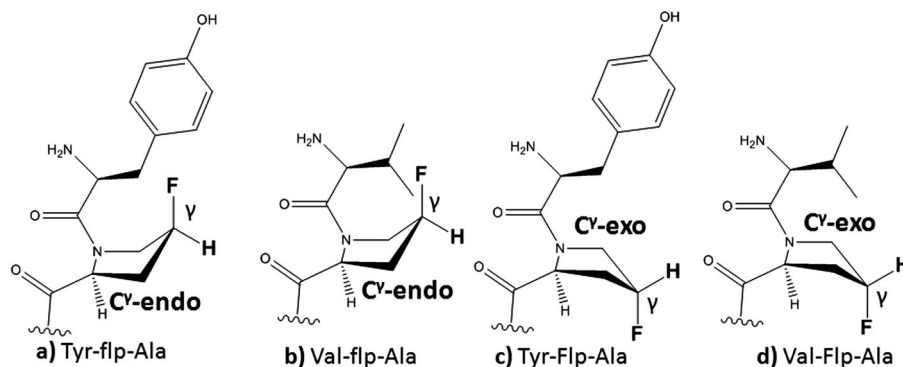


Fig. 1 Model peptides studied here and their proposed ring puckering positions: (a) Tyr-flp-Ala (*C^γ-endo*), (b) Val-flp-Ala (*C^γ-endo*), (c) Tyr-Flp-Ala (*C^γ-exo*), (d) Val-Flp-Ala (*C^γ-exo*).

Identification of the b_2 ion structures is achieved *via* gas-phase action IRMPD spectroscopy, supported by theoretical calculations enabling chemical information about each fragment ion to be obtained. Additionally, MS³ of the b_2 ions was performed to determine how the *R* to *S* change of the fluorine on the prolyl ring influences the overall stability of the b_2 ion generated in each case.

Experimental

All peptides were synthesized using standard Fmoc-solid phase synthesis described in detail elsewhere.¹⁹ Substituted Fmoc-protected 4*R*-Fluoroproline (Flp) and 4*S*-fluoroproline (flp) were purchased from BACHem while all other amino acids and synthesis reagents were purchased from EMD Biosciences, unless otherwise stated. Following cleavage from the resin, diethyl ether (Sigma-Aldrich, MO) was added to the remaining peptide solution to retain unwanted reagent impurities. The peptide was then extracted from the ether by adding an aliquot of deionized water, which was retained and purified further by two additional ether extractions. Peptide solutions for MS analysis were prepared by diluting approximately 1:100 into H₂O:ACN with 0.1% formic acid to a final concentration of 10 to 50 μ M. All solvents were purchased from Sigma-Aldrich and used without any further purification.

Action IRMPD was performed at the Centre Laser Infrarouge d'Orsay (CLIO) using a free electron laser set-up and a Bruker Esquire 3000⁺ 3-D ion trap with an electrospray ionization source. Maitre, Ortega, and co-workers have described the process in detail.^{20–22} Briefly, each precursor tripeptide was isolated in the ion trap and activated with in-trap CID to produce the b_2 ion. Subsequently, the trapped b_2 fragment ion was irradiated by the FEL at steps of 4 cm^{-1} from 1000–2000 cm^{-1} . The IRMPD spectra were produced by plotting the intensity of all fragments formed from the b_2 ion over the intensity of residual b_2 ion precursor at each wavenumber. The laser output consisted of macropulses of 9 μ s each at a repetition rate of 25 Hz. These macropulses consist of approximately 600 micropulses at 0.5–3 ps spaced out at gaps of 16 ns. With laser powers of 0.5–1 W for each micropulse, the total amount of energy per pulse was found to be about 30–100 μ J depending on the exact wavelength and power of the laser.

MS³ CID spectra for each b_2 ion were produced on a Thermo Scientific Velos Pro dual linear ion trap at The Ohio State University. Each precursor tripeptide was isolated in the low pressure cell and dissociated in the high pressure cell *via* collision induced dissociation. A collision energy of 20–23% (normalized) was used to fragment each precursor tripeptide and the b_2 ion formed was subsequently dissociated *via* CID at 23–30% normalized collision energy.

Theoretical b_2 ion structures and full tripeptide precursors were calculated using hybrid density functional theory at the B3LYP/6-311+G** basis set. A conformational search of possible structures was produced using torsional sampling of the candidate structures using the Monte Carlo Multiple Minimum (MCOMM)

with energy optimization *via* the Merck Molecular Force Field (MMFF).²³ From the list of generated structures, the 30–50 most stable unique structures of each sequence were submitted to Gaussian 09 for both optimization and frequency calculations.²⁴ The lowest energy structure for each set was found to be on average 0.5–1.5 kcal mol^{-1} lower than the next lowest structure and 7–12 kcal mol^{-1} lower than the most unstable of each unique structure found. The frequencies of these structures were scaled at 0.975 and used for comparison to the experimental IRMPD spectra produced at CLIO with artificial peak widths of 10 cm^{-1} applied.

Results and discussion

Action IRMPD spectra

A collection of the b_2 ion experimental action IRMPD (blue traces) and the corresponding theoretical spectra of lowest energy calculated diketopiperazine and oxazolone structures (red traces) is shown in Fig. 2, with Tyr-flp in Fig. 2a, Tyr-Flp in Fig. 2b, Val-flp in Fig. 2c, and Val-Flp in Fig. 2d. All four b_2 ions show stretches in the 1950 cm^{-1} region and a broad band within the region between 1580 and 1620 cm^{-1} , suggesting the possibility of multiple overlapping peaks. The stretch at 1950 cm^{-1} is indicative of an oxazolone structure as it corresponds to the amide I carbonyl stretch observed for each theoretical oxazolone spectrum in red and is notably weak in Tyr-flp. The theoretical spectra of the oxazolone ions also show multiple bands in the region \sim 1600 cm^{-1} , suggesting the broad feature observed for Val-flp, Val-Flp, and Tyr-Flp in particular could be due to the oxazolone structure. For both Tyr-Flp (b) and Val-Flp (d), these two oxazolone band regions (1950 and 1600 cm^{-1}) are the prominent features of the spectra above 1400 cm^{-1} suggesting that the dominant structure for the two Flp containing b_2 ions is the oxazolone.

For both Tyr-flp and Val-flp, there are a unique set of bands at approximately 1690 and 1750 cm^{-1} that make up a major proportion of the fragmentation efficiency signal. For Val-flp, there is a clear peak at 1760 cm^{-1} and a smaller peak at 1690 cm^{-1} adjacent to a broad feature at \sim 1600 cm^{-1} . For the calculated diketopiperazine of Tyr-flp, there are strong bands at 1750 and 1670 cm^{-1} with no similar broad feature at \sim 1600 cm^{-1} . These bands correspond to the ring carbonyl stretching (1750 cm^{-1}) and the C=N in-ring stretching (1670 cm^{-1}) of the diketopiperazine. The carbonyl stretch is in excellent agreement with the experimental band at 1760 cm^{-1} whereas the C=N stretch is slightly blue shifted in the action IRMPD spectrum. The shifting is even more pronounced for Val-flp, in that the lower diketopiperazine calculated “fingerprint” band at 1645 cm^{-1} is about 40 cm^{-1} red-shifted from the 1690 cm^{-1} experimental peak. In examining the theoretical spectra of the higher energy diketopiperazines, no pair of diketopiperazine stretches was found from the list of computed structures to match completely the two experimental peaks at 1690 and 1750 cm^{-1} .

There are no readily observable peaks for the Tyr-Flp (Fig. 2b) that match the diketopiperazine stretching region,

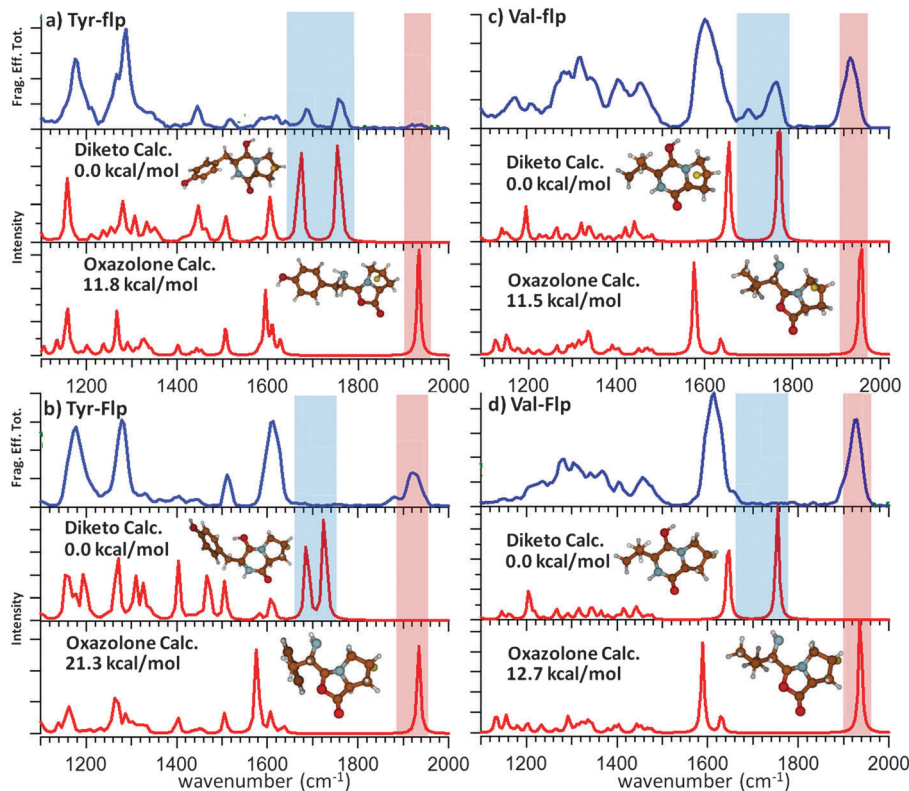


Fig. 2 Experimental IR spectra (blue) of b_2 ions from (a) Tyr-flp-Ala, (b) Tyr-Flp-Ala, (c) Val-flp-Ala, and (d) Val-Flp-Ala compared to the theoretical diketopiperazine and oxazolone structures (red) of each. The relative energies of each pair of calculated structures as well as ball and stick models of each structure are shown in the insets of each calculated spectrum. The major stretching regions for the diketopiperazine and oxazolone are highlighted in blue and red boxes, respectively, for each b_2 ion.

though a tiny peak at $\sim 1735\text{ cm}^{-1}$ may suggest a faint band in the Tyr-Flp case. In the case of Val-Flp, no discernible bands are present in the region between 1690 and 1750 cm^{-1} . There is, however, a small band at 1650 cm^{-1} adjacent and contributing to the broad feature centered at about 1615 cm^{-1} . This 1650 cm^{-1} band matches well with the C=N in-ring stretch of the calculated diketopiperazine, but the lack of a corresponding ~ 1700 feature strongly suggests that this is an oxazolone band that corresponds to the minor 1640 cm^{-1} band of the two oxazolone peaks at 1590 cm^{-1} and 1640 cm^{-1} .

From the action IRMPD spectra (summarized in Table 1), it is clear that there is little to no formation of diketopiperazine when substituting the 2nd position proline with a 4*R*-fluoroproline (Flp – high $K_{trans/cis}$), but a greater prevalence of the diketopiperazine with the fluorine in the *S* position (flp – low $K_{trans/cis}$). The *S*-substitution retains the oxazolone bands in

Tyr-flp (Fig. 2a), as shown by the presence of a weak amide I carbonyl vibrational stretch, yet the diketopiperazine structure becomes the dominant species. This is in contrast to the Val-Xxx systems (Fig. 2c and d), where both substitutions retain large oxazolone bands from 1930 – 1950 cm^{-1} with the expected diketopiperazine peaks at 1700 and 1760 cm^{-1} observed only in the Val-flp case. Thus while the *S*-fluoro substitution promotes formation of the diketopiperazine structure for both Tyr-flp and Val-flp, in the case of Val-flp the results suggest that a substantial proportion of ions retain a *trans* peptide bond and form the oxazolone structure. Additionally, it should be noted that for all four b_2 ions, the diketopiperazine was found to be the lowest energy structure (inset of Fig. 2). Each oxazolone was at least 11 kcal mol^{-1} higher in energy than the diketopiperazine with the oxazolone of Tyr-Flp 21 kcal mol^{-1} higher in energy than the diketopiperazine. Because Tyr-Flp was found to show

Table 1 Major and minor stretches of each b_2 ion and the percentage of each relative to the most intense stretch in the fingerprinting region. The final column suggests the major structure based on the contributions of each identifying stretch

b_2 identity	Oxazolone stretch	Diketopiperazine stretches		
	Amide I C=O	Ring C=O	In-ring C=N	Major structure
Tyr-flp	Minor@ 1925 cm^{-1} (13%)	Major@ 1760 cm^{-1} (100%)	Major@ 1695 cm^{-1} (75%)	Diketo
Tyr-Flp	Major@ $1925/1890\text{ cm}^{-1}$ (100%)	Minor@ 1750 cm^{-1} (10%)	Not observed	Oxaz
Val-flp	Major@ 1905 cm^{-1} (100%)	Major@ 1740 cm^{-1} (40%)	Moderate@ 1690 cm^{-1} (20%)	Diketo/oxaz
Val-Flp	Major@ 1920 cm^{-1} (100%)	Not observed	Not observed	Oxaz

only oxazolone stretches in its IRMPD spectrum this suggests that the absolute energy of the resulting b_2 ion is not a factor in its formation, which is consistent with the general understanding that fragmentation in MS/MS is kinetically driven.

MS³ b_2 ion fragmentation

Fig. 3 shows the b_2 MS³ CID spectra ($MH^+ \rightarrow b_2 \rightarrow$ fragments) of Val-flp-Ala (Fig. 3a) and Val-Flp-Ala (Fig. 3b) produced in a Thermo Scientific Velos Pro dual cell linear ion trap. Both spectra were collected using the same 23% relative CID collision energy for the precursor and b_2 ion. The top spectrum, for Val-flp-Ala, contains a residual precursor b_2 ion at approximately 30% normalized CID intensity and the a_2 ion (loss of CO) as the most intense peak. The HF loss from the a_2 and the [HF + CO] loss from a_2 also produce dominant peaks at this fragmentation energy. The b_2 ion undergoes NH_3 loss, HF loss, an imine loss to produce m/z 144, as well as combinations of these losses (a_2 -HF-CO- NH_3 and b_2 -imine-CO). Additionally, both the flp and Val iminium ion fragments are observed at m/z 88 and 72, respectively. In the case of the Val-Flp b_2 ion, significantly fewer high intensity fragments are observed. Again, the most intense peak in the spectrum is the a_2 ion at m/z 187, followed by the imine loss fragment. Other fragments present include the b_2 -H₂O, a peak at m/z 171 believed to be a CO₂ loss from the b_2 , a CO loss from the b_2 -imine fragment, and the two peptide iminium fragments Val_{imm} and Flp_{imm}. Significantly, for the Val-Flp b_2 ion, no peak of reasonable intensity which corresponds to an HF loss is observed. This may be directly due to the

C^{γ} -*exo* ring conformation of the Val-Flp b_2 ion, in which the substituent is positioned in the proline ring such that it is inaccessible to any other functional groups within the small, inflexible fragment ion. Conversely, the C^{γ} -*endo* conformation of the Val-flp b_2 ion makes it readily accessible to H-bonding with the other functional groups, allowing many possible fluorine interactions to occur resulting in HF loss, as observed (b_2 -HF, a_2 -HF, a_2 -HF-CO, a_2 -HF-CO- NH_3).

Fig. 4 presents the MS³ spectral comparison for the Tyr-flp and Tyr-Flp b_2 ions. The IRMPD spectra above show that diketopiperazine dominates clearly for Tyr-flp while only oxazolone was readily observed for Tyr-Flp, which justifies the sharp differences in MS³ of the Tyr-flp and Tyr-Flp b_2 ions. A distinct feature of the Tyr-flp b_2 ion is that its most intense fragment is the Tyr iminium ion rather than the a_2 , which is the most intense for Tyr-Flp, Val-flp, and Val-Flp. Because it is most facile to form the a_2 through the oxazolone structure *via* a carbonyl loss,^{25,26} the fact that it is the least intense for the Tyr-flp b_2 correlates with the action IRMPD results in which the oxazolone band stretches were the least intense for Tyr-flp.

Significantly, it is clear that there is more residual b_2 in the spectra of Val-flp and Tyr-flp than the corresponding Flp-containing ion precursors, where the b_2 ion intensity has almost disappeared. This suggests that the *S* position fluorine of flp (C^{γ} -*endo*) is adding stability to the b_2 ion compared to *R* position fluorine of Flp (C^{γ} -*exo*). It may also be that the ring puckering is retained in the oxazolone structure and is contributing to the very different spectra corresponding to the

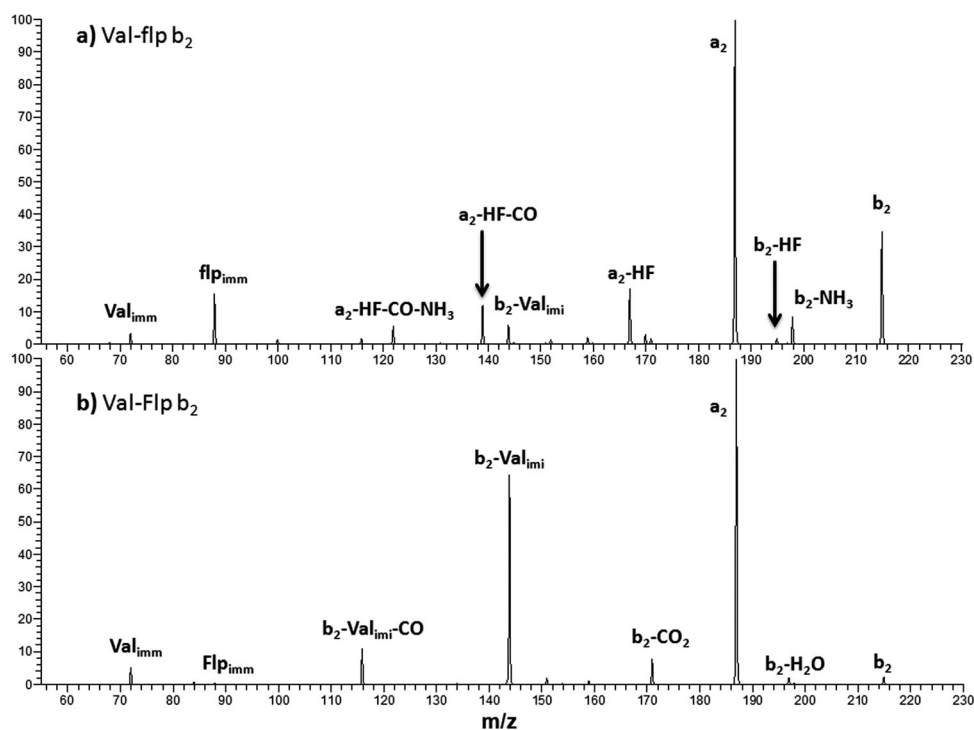


Fig. 3 MS³ of b_2 ions of (a) Val-flp-Ala and (b) Val-Flp-Ala performed on a Velos Pro linear ion trap. Precursor tripeptides were isolated and fragmented at 23% CID collision energy followed by isolation and fragmentation of each b_2 at m/z 215 at the same collision energy. The -Val_{imi} label indicates the loss of the valine neutral imine while Val_{imm}, flp_{imm}, and Flp_{imm} labels indicate the iminium (immonium) ions of valine, *S*-fluoroproline, and *R*-Fluoroproline, respectively.

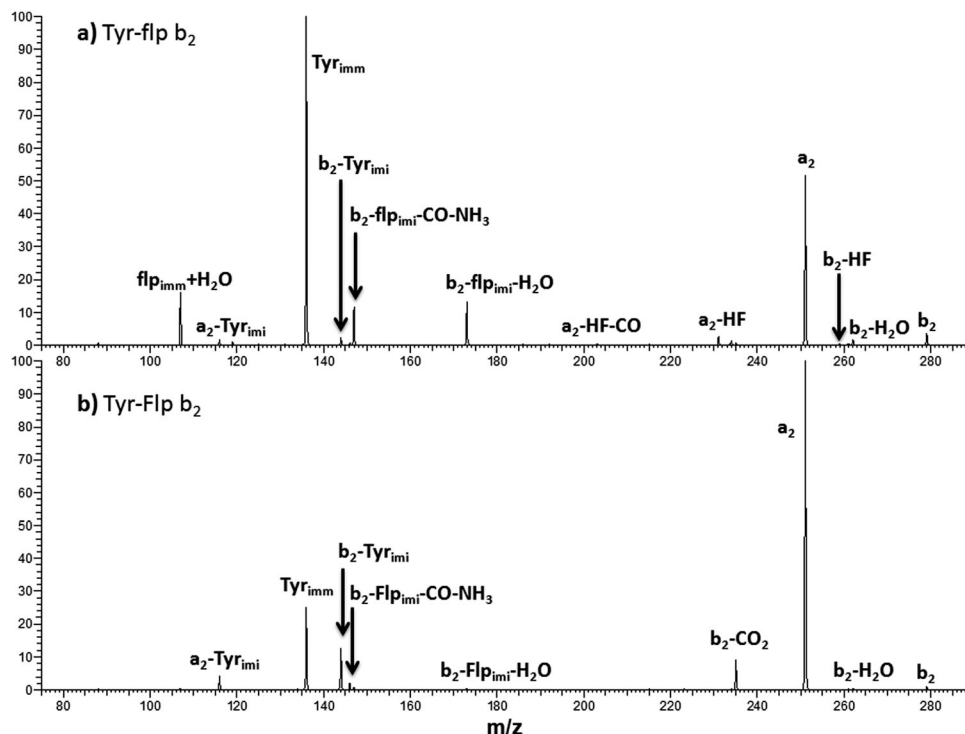


Fig. 4 MS^3 of b_2 ions of (a) Tyr-flp-Ala and (b) Tyr-Flp-Ala performed on a Velos Pro linear ion trap. Precursor tripeptides were isolated and fragmented at 20% HCD collision energy followed by isolation and fragmentation of each b_2 ion at m/z 279 with 25% CID collision energy. The $-Tyr_{imi}$, $-flp_{imi}$, and $-Flp_{imi}$ labels indicate losses of the tyrosine, *S*-fluoroproline, and *R*-Fluoroproline imines while Tyr_{imm} , flp_{imm} , and Flp_{imm} labels indicate the iminium ions of tyrosine, *S*-fluoroproline, and *R*-Fluoroproline, respectively.

two differently substituted prolyl ring residues. The stability of these fragment ions could be in part due to the ability of the fluorine substituent to participate in further fragmentation pathways of the molecule, making the inherent stability of the fragments dependent on the stereochemistry of the ring substituents. This explains why there is such a large difference in remaining precursor between the Val-Flp and Val-flp b_2 ions at the exact same MS^3 fragmentation energy. Despite the fact that the b_2 ion appears to be more stable for Val-flp there are, however, also a significantly greater number of different fragments for this b_2 ion. Interestingly, this is less of a feature in the tyrosine dissociation comparison (Fig. 4), where the two precursors are both almost completely gone.

Comparison to solution phase trends *via* gas phase theoretical optimization

The experimental action IRMPD and MS^3 spectra shown above define a clear trend for oxazolone/diketopiperazine ratios for *S*-substituted flp that agree with the $K_{trans/cis}$ trend found by Shoulders *et al.* using solution-phase 1-D proton NMR.⁹ For the *S*-substituted flp second position tripeptides of Tyr-flp-Ala and Val-flp-Ala, the *cis* peptide bond is more likely both in solution and in the gas-phase experiments presented here, which explains why the diketopiperazine is present in greater proportions for these substitutions. As the $K_{trans/cis}$ trend observed previously in solution correlates with the peptide bond conformation necessary for diketopiperazine formation, it is desirable to also determine whether the prolyl ring puckering observed in the solution-phase is preserved the gas-phase. Additionally, while no experimental

data were collected for the precursor tripeptides, it is critical to determine their most likely structures *in silico* as the structure of each b_2 ion is formed directly from its tripeptide precursor. The lowest energy N-protonated tripeptides (a) Tyr-flp-Ala, (b) Val-flp-Ala, (c) Tyr-Flp-Ala, and (d) Val-Flp-Ala, calculated with DFT, are shown in Fig. 5. As shown in the boxed region in Fig. 5 on the prolyl ring section of the molecule, the fluorine substitution on the 4th position of the prolyl ring causes the ring to pucker towards the side on which the fluorine is added. This was observed previously by Crestoni *et al.* for Hyp and hyp *in silico* in addition to Panasik *et al.* in solution-phase studies of collagen and Ac-Xxx-OME where Xxx = Pro, flp, Flp, hyp, or Hyp.^{5,15} For Tyr-flp-Ala and Val-flp-Ala in Fig. 5a and c, the ring orients into a *C-endo* position and the fluorine is involved in a hydrogen bond with the 3rd amide nitrogen (alanine). For Tyr-Flp-Ala and Val-Flp-Ala, the ring orients itself into the *C'-exo* conformation, away from the majority of the other functional groups. Likewise, it appears that the strain of this ring results in less hydrogen bonding for the N-terminus and an overall lack of stability for the tripeptide (3 kcal mol⁻¹ higher in energy). Val-flp-Ala is approximately 2.6 kcal mol⁻¹ lower in energy than Val-Flp-Ala and Tyr-flp-Ala is 2.4 kcal mol⁻¹ lower than Tyr-Flp-Ala.

Previous studies on the ring puckering of proline considered only whole peptides and not the fragments corresponding to the b_2 ion, hence, Gaussian structures of the oxazolone and diketopiperazine fragments were also studied here to determine if ring puckering would be retained in their gas-phase formation. Fig. 6 shows DFT optimized lowest energy structures of the oxazolones (Fig. 6a–d) and diketopiperazines (Fig. 6e–h)

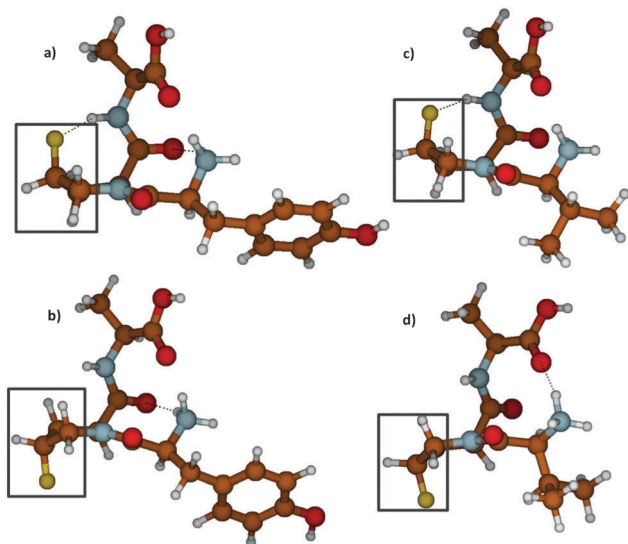


Fig. 5 (a) Tyr-flp-Ala, (b) Tyr-Flp-Ala, (c) Val-flp-Ala, and (d) Val-Flp-Ala protonated tripeptide models calculated at the B3LYP/6-31+G** with Gaussian 09, with fluorine indicated in gold. Using gas phase conditions, the ring puckering of the *R* and *S* fluoroproline structures form the *C'*-endo and *C'*-exo conformations that are present in solution.¹³ Prolyl rings for all fluoroprolines are boxed in black and are oriented in a full side view to most clearly display the ring puckering.

of Tyr-flp, Tyr-Flp, Val-flp and Val-Flp. As shown in the MS³ data above, the *R* and *S* position of the fluoro-substitution has a large effect on not only the precursor peptide which forms the b₂ but on the b₂ ion itself. Here the theoretical structures show that the ring puckering is retained independent of whether the ion is oxazolone or diketopiperazine. Furthermore, the models containing flp in the second position explain the HF loss observed for Tyr-flp and Val-flp and the absence of these fragments for the Flp analogues in MS³ experiments (Fig. 3b and 4b, respectively). For Flp containing oxazolone or diketopiperazine (Fig. 6b, d, f, and h), no other functional group can participate in an internal reaction with the fluorine on the prolyl ring without a

significant strain on the molecule, resulting in little to no reactivity of this substituent after formation of the b₂ product ion. In contrast for flp (Fig. 6a, c, e, and g), H-bonding to the fluorine substituent is possible and allows for reactions resulting in the HF-loss, as seen in the flp-containing b₂ ions above in the MS³ section (Fig. 3 and 4). The theoretical calculations coupled with the data from the IRMPD and MS³ allows for a confirmation of not only the structural differences of the *R/S* prolyl substitutions, but also helps in elucidating the reasons for why those fragmentation and vibrational differences occur in the gas-phase.

The influence of histidine in the first position on b₂ ions of His-Flp-Ala and His-flp-Ala

A set of IRMPD and MS³ data from the His-Flp-Ala and His-flp-Ala tripeptides was also run and is shown in the supplementary information (ESI,† Fig. S1 and S2). The identity of the b₂ ions from this particular set was shown to be independent of the stereochemistry of the 4th position of the prolyl ring and both His-flp and His-Flp were clearly observed to be exclusively diketopiperazine. Additionally the fragments formed were the same for both His-Flp and His-flp with the exception of the HF loss, a sign of both b₂ populations having the same structure. Previous work by Gucinski and coworkers has already confirmed the exclusivity of the diketopiperazine structure in His-Pro b₂ ions and the ESI† suggest that despite the ability of the fluoroproline to increase the $K_{trans/cis}$ of the peptide bond this effect does not overcome the effect of the imidazole of the histidine on the resulting b ion structure.¹⁷

Conclusions

The results above reveal that the 4-substitution of the prolyl ring in the second position of tripeptides has a significant effect on relative populations of diketopiperazine and oxazolone in b₂ ion fragments. From action IRMPD spectra, distinct trends were found for Tyr and Val with Flp or flp in the second position. In the case of tyrosine in the first position (*i.e.* Tyr-Flp vs. Tyr-flp), there is a stark contrast in

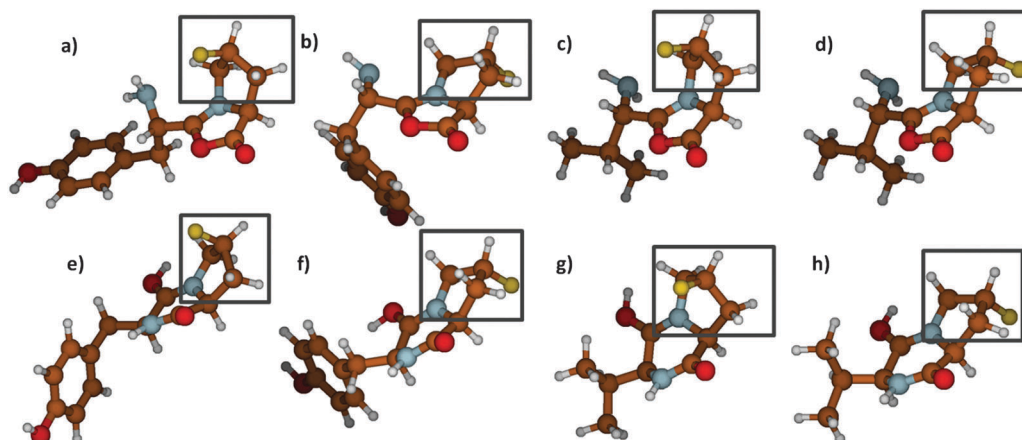


Fig. 6 Protonated oxazolone b₂ models (top row) of (a) Tyr-flp, (b) Tyr-Flp, (c) Val-flp, (d) Val-Flp and their corresponding diketopiperazine b₂ ion models directly below each oxazolone model (e–h) calculated at the B3LYP/6-311+G** level with Gaussian 09 with prolyl rings boxed in black. For these two fragment structures, as with the tripeptide precursors, the ring pucker conformations of the *R* and *S* fluoroproline substitutions are retained.

vibrational stretches with oxazolone the only structure observed for Tyr-Flp and the diketopiperazine the dominant structure for Tyr-flp, with only a minor abundance of oxazolone. With valine in the first position, the dominant structure remained the oxazolone in both cases but a diketopiperazine population was also present for Val-flp. The general trend here also carried over for the MS³ spectra of each population of b₂ ions. For Tyr-Flp and Tyr-flp, the differences resulting from b₂ activation, including both precursor abundances and fragment types, was considerable, implying different structures for the two populations. Again, the valine subset showed greater similarities between Flp and flp substitutions but with a significant difference in the ammonia loss and interestingly an HF loss, a trend thought to be a result of the configuration of the fluorine on the ring and the corresponding ring puckering.

The ion structure dependence for valine and tyrosine in the first-position correlated extremely well to the *K*_{trans/cis} prevalence previously found in solution-phase studies of these prolyl substituted residues. From the data presented here, it seems apparent that the nature of the first peptide bond directly influences the formation of diketopiperazine in gas-phase fragmentation into b₂ ions. Second position substitutions of flp and Flp produced a primarily *cis* or *trans* b₂ ion, matching those trends previously observed in solution. Additionally, the *R* and *S* fluoroproline substitutions caused different degrees of b₂ precursor dissociation at the same collision energy. By moving the fluorine on the gamma carbon of the prolyl ring from the *S* to the *R* configuration there is a significant change to both the stability of the b₂ ion and identity of its subsequent MS³ fragments. The position of the fluoro substitution is also seen to directly influence the ring-puckering of both the gas-phase precursors and their b₂ ions, whether oxazolone or diketopiperazine, which further supports the relationship of these peptide ions to the effects of prolyl ring substitution in solution-phase peptide chemistry.

Acknowledgements

The authors would like to thank Vincent Steinmetz and Philippe Maitre at the Laboratoire de Chimie Physique in Orsay, France for use of and assistance with the CLIO experimental facilities. Additional thanks go to The Ohio State University and the Ohio Supercomputing Center.

References

- B. Balta, V. Aviyente and C. Lifshitz, *J. Am. Soc. Mass Spectrom.*, 2003, **14**, 1192–1203.
- C. Bleiholder, S. Suhai, A. G. Harrison and B. Paizs, *J. Am. Soc. Mass Spectrom.*, 2011, **22**, 1032–1039.
- B. Paizs and S. Suhai, *Mass Spectrom. Rev.*, 2005, **24**, 508–548.
- D. Pal and P. Chakrabarti, *J. Mol. Biol.*, 1999, **294**, 271–288.
- N. Panasik, E. S. Eberhardt, A. S. Edison, D. R. Powell and R. T. Raines, *Int. J. Pept. Protein Res.*, 1994, **44**, 262–269.
- W. L. Jorgensen and J. Gao, *J. Am. Chem. Soc.*, 1988, **110**, 4212–4216.
- A. C. Gucinski, J. Chamot-Rooke, V. Steinmetz, A. Somogyi and V. H. Wysocki, *J. Phys. Chem. A*, 2013, **117**, 1291–1298.
- L. L. Smith, K. A. Herrmann and V. H. Wysocki, *J. Am. Soc. Mass Spectrom.*, 2006, **17**, 20–28.
- M. D. Shoulders, J. A. Hodges and R. T. Raines, *J. Am. Chem. Soc.*, 2006, **128**, 8112–8113.
- M. D. Shoulders, K. J. Kamer and R. T. Raines, *Bioorg. Med. Chem. Lett.*, 2009, **19**, 3859–3862.
- Y. C. Chiang, Y. J. Lin and J. C. Horng, *Protein Sci.*, 2009, **18**, 1967–1977.
- M. D. Shoulders, K. A. Satyshur, K. T. Forest and R. T. Raines, *Proc. Natl. Acad. Sci. U. S. A.*, 2010, **107**, 559–564.
- W. Kim, K. I. Hardcastle and V. P. Conticello, *Angew. Chem., Int. Ed.*, 2006, **45**, 8141–8145.
- K. L. Gorres, R. Edupuganti, G. R. Krow and R. T. Raines, *Biochemistry*, 2008, **47**, 9447–9455.
- M. E. Crestoni, B. Chiavarino, D. Scuderi, A. Di Marzio and S. Fornarini, *J. Phys. Chem. B*, 2012, **116**, 8771–8779.
- T. G. Flick, I. D. G. Campuzano and M. D. Bartberger, *Anal. Chem.*, 2015, **87**, 3300–3307.
- A. C. Gucinski, J. Chamot-Rooke, E. Nicol, A. Somogyi and V. H. Wysocki, *J. Phys. Chem. A*, 2012, **116**, 4296–4304.
- K. M. Thomas, D. Naduthambi and N. J. Zondlo, *J. Am. Chem. Soc.*, 2006, **128**, 2216–2217.
- E. Atherton and R. C. Sheppard, *Solid-Phase Peptide Synthesis: A Practical Approach*, Oxford University Press, Oxford, UK, 1989.
- J. Lemaire, P. Boissel, M. Heninger, G. Mauclaire, G. Bellec, H. Mestdagh, A. Simon, S. L. Caer, J. M. Ortega, F. Glotin and P. Maitre, *Phys. Rev. Lett.*, 2002, **89**, 273002.
- L. Mac Aleese, A. Simon, T. B. McMahon, J. M. Ortega, D. Scuderi, J. Lemaire and P. Maitre, *Int. J. Mass Spectrom.*, 2006, **249**, 14–20.
- P. Maitre, S. Le Caer, A. Simon, W. Jones, J. Lemaire, H. N. Mestdagh, M. Heninger, G. Mauclaire, P. Boissel, R. Prazeres, F. Glotin and J. M. Ortega, *Nucl. Instrum. Methods Phys. Res., Sect. A*, 2003, **507**, 541–546.
- MacroModel, in, Schrödinger, LLC, New York, NY, 2012.
- M. J. Frisch, G. W. Trucks, H. B. Schlegel, G. E. Scuseria, M. A. Robb, J. R. Cheeseman, G. Scalmani, V. Barone, B. Mennucci, G. A. Petersson, H. Nakatsuji, M. Caricato, X. Li, H. P. Hratchian, A. F. Izmaylov, J. Bloino, G. Zheng, J. L. Sonnenberg, M. Hada, M. Ehara, K. Toyota, R. Fukuda, J. Hasegawa, M. Ishida, T. Nakajima, Y. Honda, O. Kitao, H. Nakai, T. Vreven, J. A. Montgomery, Jr., J. E. Peralta, F. Ogliaro, M. Bearpark, J. J. Heyd, E. Brothers, K. N. Kudin, V. N. Staroverov, R. Kobayashi, J. Normand, K. Raghavachari, A. Rendell, J. C. Burant, S. S. Iyengar, J. Tomasi, M. Cossi, N. Rega, J. M. Millam, M. Klene, J. E. Knox, J. B. Cross, V. Bakken, C. Adamo, J. Jaramillo, R. Gomperts, R. E. Stratmann, O. Yazyev, A. J. Austin, R. Cammi, C. Pomelli, J. W. Ochterski, R. L. Martin, K. Morokuma, V. G. Zakrzewski, G. A. Voth, P. Salvador, J. J. Dannenberg, S. Dapprich, A. D. Daniels, Ö. Farkas, J. B. Foresman, J. V. Ortiz, J. Cioslowski and D. J. Fox, *Gaussian 09*, Wallingford, CT, 2009.
- T. Yalcin, C. Khouw, I. G. Csizmadia, M. R. Peterson and A. G. Harrison, *J. Am. Soc. Mass Spectrom.*, 1995, **6**, 1165–1174.
- T. Yalcin, I. G. Csizmadia, M. R. Peterson and A. G. Harrison, *J. Am. Soc. Mass Spectrom.*, 1996, **7**, 233–242.